Supplementary figures for:

Bacterial flagellar motor PL-ring disassembly subcomplexes are widespread and ancient

Mohammed Kaplan[a], Michael J. Sweredoski[a], João P.G.L.M. Rodrigues[b], Elitza I. Tocheva[a,1], Yi-Wei Chang[a,2], Davi R. Ortega[a], Morgan Beeby[a,3] and Grant J. Jensen[a,c,4]

[a]Division of Biology and Biological Engineering, California Institute of Technology, Pasadena, CA 91125, USA

[b]Department of Structural Biology, Stanford University, Stanford, CA, USA

[1]Present address: Department of Microbiology and Immunology, Life Sciences Institute, The University of British Columbia, Vancouver, BC V6T 1Z3, Canada

[2]Present address: Department of Biochemistry and Biophysics, Perelman School of Medicine, University of Pennsylvania, Philadelphia, PA 19104, USA

[3]Present address: Department of Life Sciences, Imperial College London, South Kensington Campus, London SW7 2AZ, UK

[c]Howard Hughes Medical Institute, California Institute of Technology, Pasadena, CA 91125, USA

[4]Corresponding author: Jensen@caltech.edu

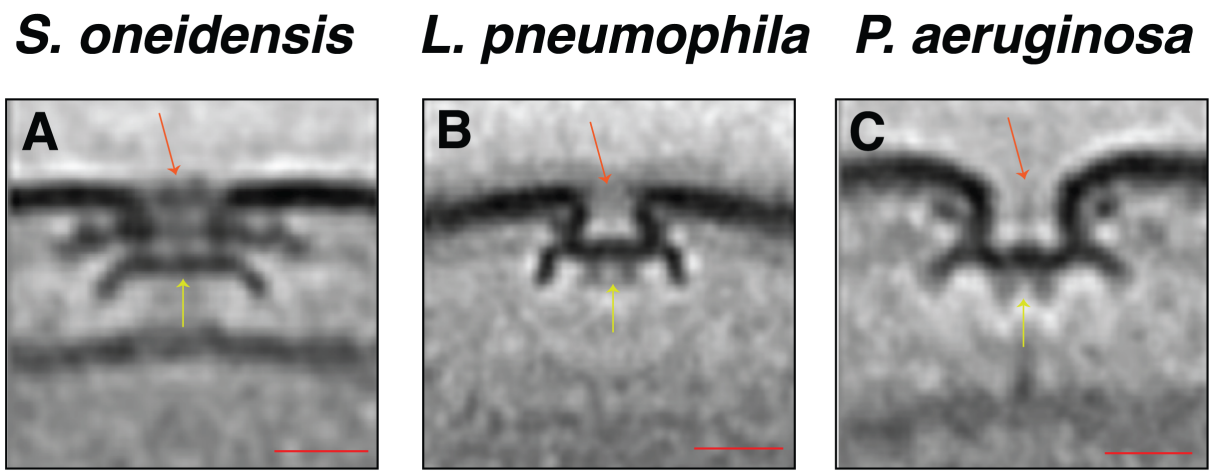

Figure S1: Central slices through sub-tomogram averages of PL-subcomplexes in *S. oneidensis* (**A**), *L. pneumophila* (**B**) and *P. aeruginosa* (**C**). Orange arrows indicate the discontinuity in the outer membrane. Note the presence of two densities below the orange arrow in *S. oneidensis*. Yellow arrows point to the plug densities in these structures. Scale bars are 20 nm. These structures are reproduced from Figure 1C, H, and M in Kaplan M., Subramanian P., Ghosal D., Oikonomou CM, Pirbadian S., Starwalt-Lee R., Mageswaran SK, Ortega DR, Gralnick JA, El-Naggar MY, Jensen GJ (2019) In situ imaging of bacterial flagellar motor disassembly and assembly processes. EMBO J 38: el00957. See ref. (7) in the main text.

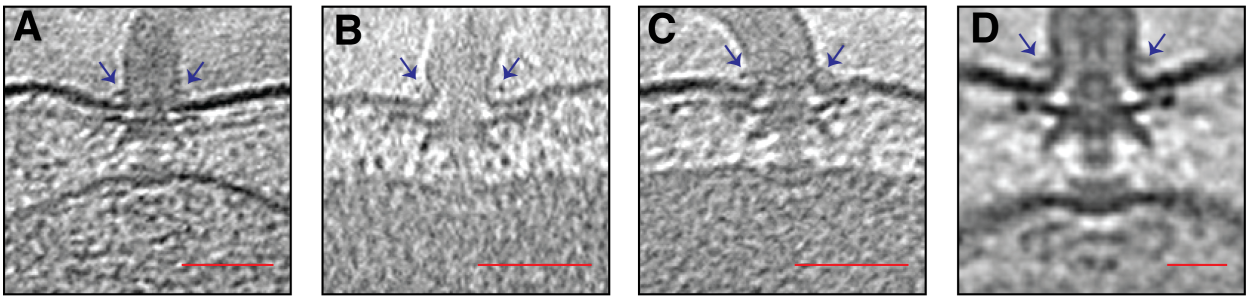

Figure S2: A, B and C) Slices through electron cryo-tomograms of *V. harveyi* with the blue arrows highlighting the presence of an extracellular ring at the bending of the outer membrane to form the sheath that surrounds the flagellar filament. Scale bars are 50 nm. **D)** A central slice through the sub-tomogram average of the sheathed flagellar motor of *V. harveyi* obtained by averaging five particles only to indicate the presence of the extracellular ring (blue arrows). Scale bar is 20 nm.

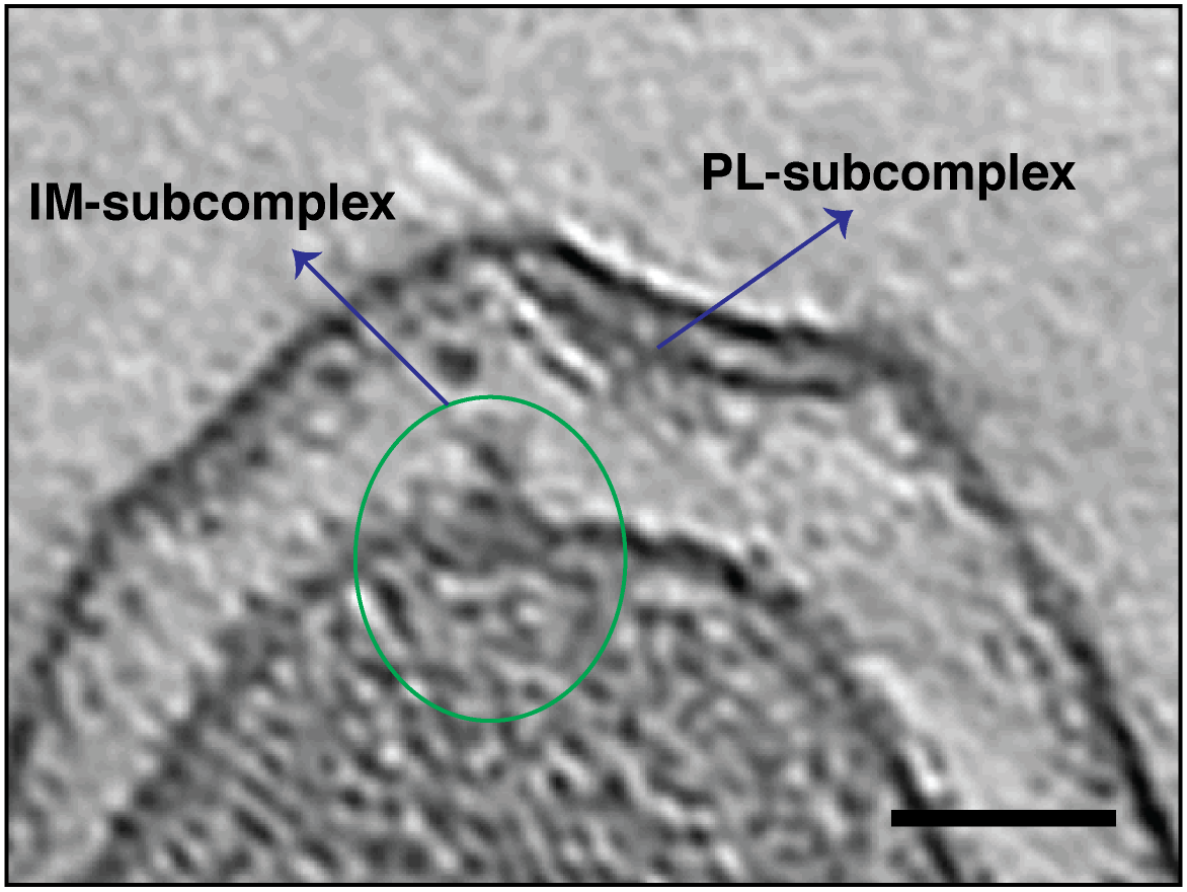

Figure S3: A slice through electron cryo-tomogram of a *C. jejuni* cell illustrating the presence of an inner-membrane (IM) associated subcomplex (green circle) next to the outer-membrane associated PL-subcomplex. This is a different slice of the same example shown in Figure 4 E and F. Note that a similar observation has been recently described for *L. pneumophila* (see ref. (7) in the main text). Scale bar is 50 nm.

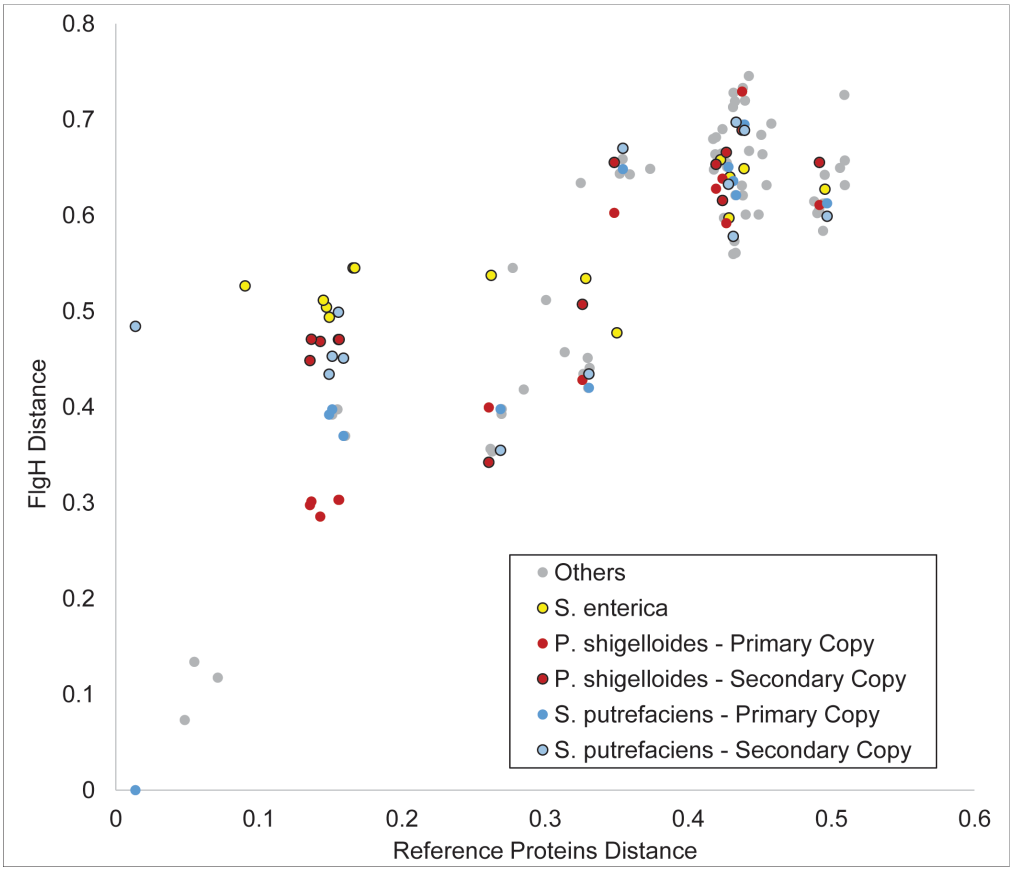

Figure S4: A scatter plot of the pairwise sequence distance of the investigated species based on concatenated 25 reference proteins and the L-ring protein, FlgH. In this plot both copies of FlgH proteins found in *S. putrefaciens* and *P. shigelloides* are used and highlighted. Interestingly, *Salmonella* FlgH protein is more divergent than expected based on the concatenated reference proteins distance. Note that in Figure 5A only the primary copies of *S. putrefaciens* and *P. shigelloides* are used. The X- and Y-axes in this plot have arbitrary units.

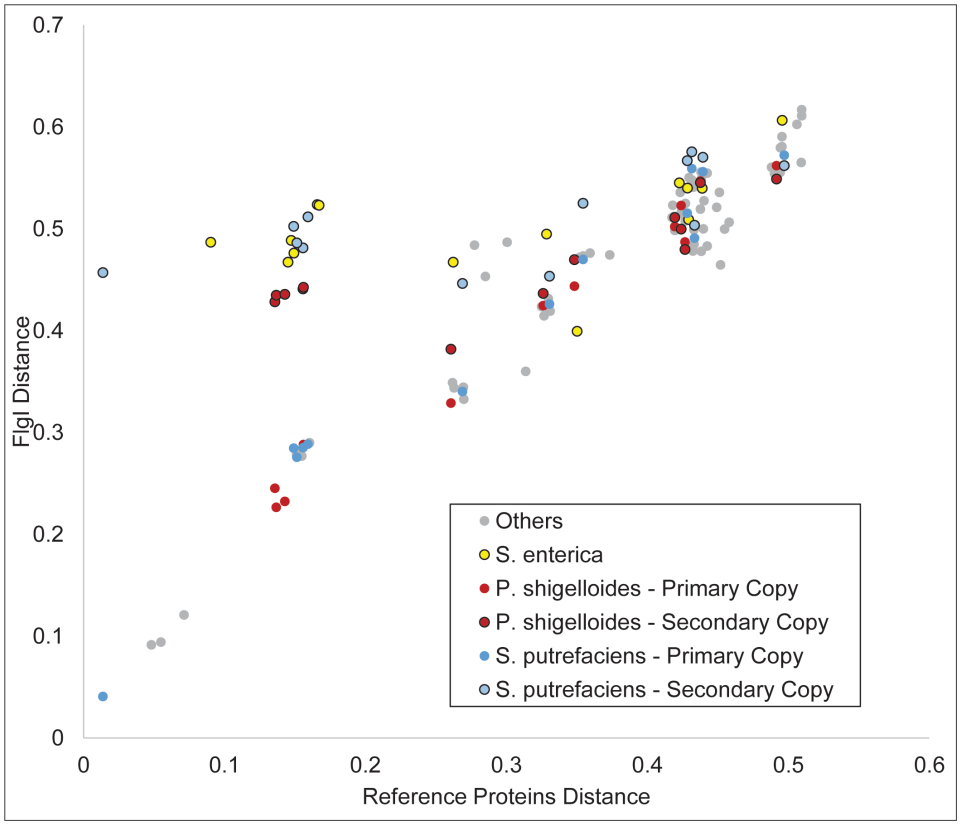

Figure S5: A scatter plot of the pairwise sequence distance of the investigated species based on concatenated 25 reference proteins and the P-ring protein, FlgI. In this plot both copies of FlgI proteins found in *S. putrefaciens* and *P. shigelloides* are used and highlighted. Interestingly, *Salmonella* FlgI protein is more divergent than expected based on the concatenated reference proteins distance. Note that in Figure 5B only the primary copies of *S. putrefaciens* and *P. shigelloides* are used. The X- and Y-axes in this plot have arbitrary units.

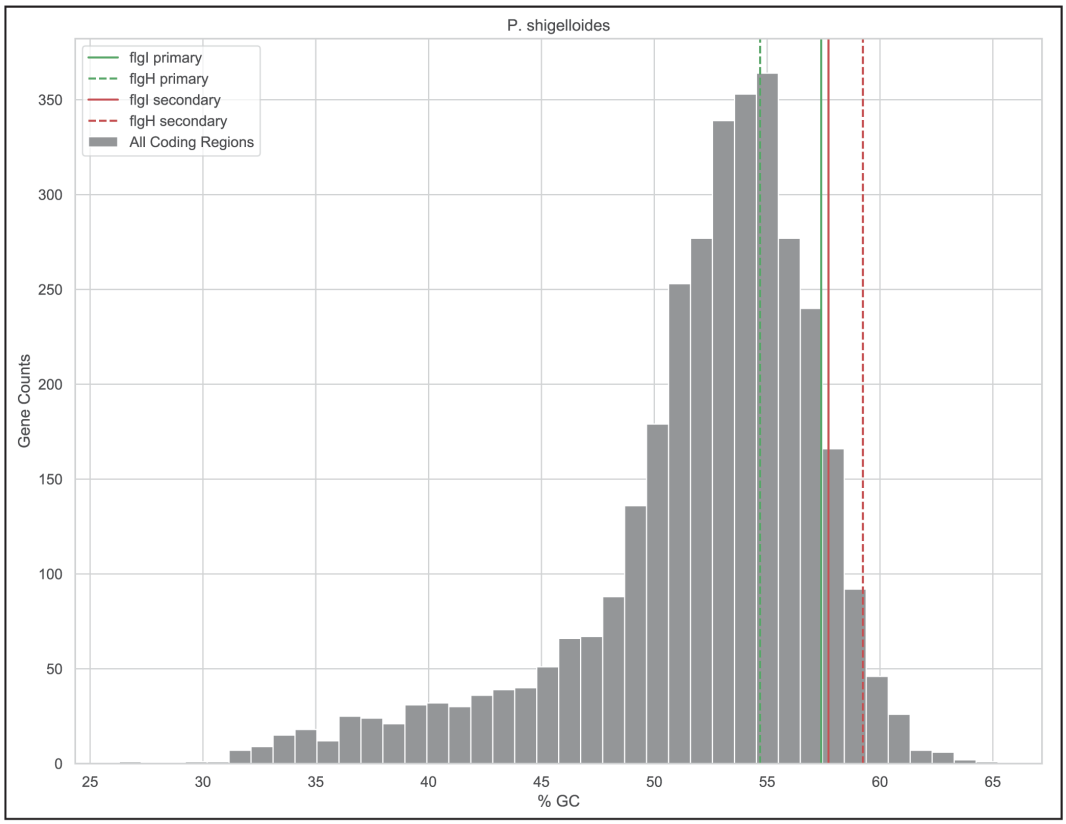

Figure S6: GC-content analysis was calculated for every gene within *P. shigelloides* and plotted as a histogram. GC contents of both primary and secondary copies of *flgH* and *flgI* are overlaid.

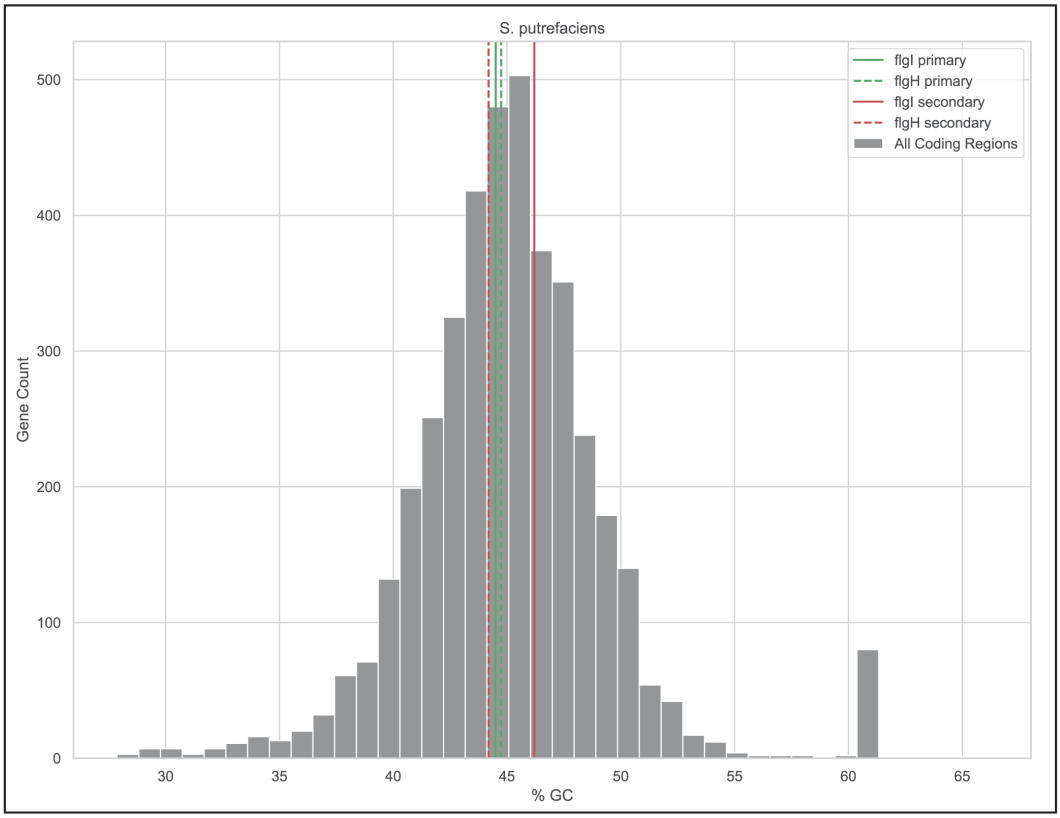

Figure S7: GC-content analysis was calculated for every gene within *S. putrefaciens* and plotted as a histogram. GC contents of both primary and secondary copies of *flgH* and *flgI* are overlaid.

Movie legend:

Movie S1: Electron cryo-tomogram of a *C. jejuni* cell illustrating the presence of an inner-membrane associated subcomplex in the vicinity of PL-subcomplex.